RELATIONSHIP BETWEEN ALUMINA AND CHLORIDE CONTENT ON THEIR PHYSICAL AND CORROSION RESISTANCE PROPERTIES OF CONCRETE

K. Thangavel*, S. Muralidharan, V. Saraswathy

Corrosion Protection Division, Central Electrochemical Research Institute, Karaikudi 630 006, Tamilnadu, India

Ki Yong Ann and L. Balamurugan

School of Civil and Environmental Engineering, Yonsei University, Seoul, 120-749, Republic of Korea

الخلاصــة:

تمت - في هذه الورقة - دراسة العلاقة بين محتوى الألومينا والكلوريد على الخصائص الفيزيائية ومقاومة التآكل للخرسانة العادية OPC.

تشكل ملح Friedel’s في الموقع في الخرسانة العادية OPC من خلال إضافة نسب مختلفة من الألومينا (1% to 15%) مع 1 % cacl2 . وقد كشفت بيانات قوه الضغط أن إضافة AL2O3 تزيد من القوة المبكرة للخرسانة.

وقد أظهر تشكل ملح Friedel’s حتى AL2O3 %5 أقصى قوة ضغط للخرسانة . كما أظهر اختبار نفاذية ايون الكلوريد السريع (RCPT) أن الشحنة المارة للخرسانة العادية OPC عند AL2O3 %5 أبدت انخفاضا مقداره %50 في الكولومب . وأشار اختبار الجهد 12v إلى زيادة تدريجية في تدفق التيار الأنودي وزمن التأخير المأخوذ لبداية التشقق حتى إضافه AL2O3 %5 .و كانت معطيات الجهد مقابل الزمن من دراسة خلية التآكل قد حافظت على حديد التسليح الموجود داخل الخرسانة العادية opc حتى AL2O3 %5 خلال فترة التعرض لمدة 12 شهرا.

وفي المقابل, فإن تيار الخلية أيضا قد تناقص (50%) في الخرسانة العادية OPC عند مستوى AL2O3 %5. وكشف المسح مايكروجراف عن تشكل كثيف لملح Friedel’s عند مستوى AL2O3 %5. أن نمط XRD عن مستوى AL2O3 %5 أكد أيضا على وجود قدر أكبر من أملاح Friedel’s . أن النسبة المثلى للألمونيا لتشكيل أملاح Friedel’s في الخرسانة العادة OPC بخصائص محسنه وجدت أنها %5 .

*Corresponding Author:

E-mail: thangam12156@yahoo.co.in

Paper Received February 2, 2009; Paper Revised 30, 2009; Paper Accepted December 21, 2009

ABSTRACT

The relationship between alumina and chloride content on the physical and corrosion resistance properties of OPC concrete was studied. Friedel's salt was formed *in situ* in OPC concrete by the addition of various percentages of alumina (1% to 15%) along with 1% $CaCl_2$. The compressive strength data revealed that the addition of Al_2O_3 increased the early strength of concrete. The Friedel's salt formation up to 5% Al_2O_3 showed maximum compressive strength. The Rapid Chloride Ion Permeability Test (RCPT) revealed that the quantity of electrical charge passed for OPC concrete at 5% Al_2O_3 showed a 50% reduction in coulombs. The 12V impressed voltage test indicated a gradual increase in anodic current flow and delayed time taken for initial crack up to 5% Al_2O_3 addition. Potential *vs* time data from macrocell corrosion studies maintained the passivity of steel embedded in OPC concrete up to 5% Al_2O_3 throughout the exposure period of 12 months. Correspondingly, the macrocell current was also considerably reduced (50%) in OPC concrete at the 5% Al_2O_3 level. Scanning electron micrographs revealed a denser formation of Friedel's salt at the 5% Al_2O_3 level. The XRD pattern at the 5% Al_2O_3 level also confirmed the existence of a greater amount of Friedel's salt. The optimum percentage of alumina for the formation of Friedel's salt in OPC concrete with improved properties was found to be 5%.

Key words: Friedel's salt formation, reinforcement corrosion, concrete, alumina

RELATIONSHIP BETWEEN ALUMINA AND CHLORIDE CONTENT ON THEIR PHYSICAL AND CORROSION RESISTANCE PROPERTIES OF CONCRETE

1. INTRODUCTION

Several mechanisms exist for chloride binding during cement hydration: these include the generally recognized mechanism involving the formation of Friedel's salt (FS). FS is $3CaO \cdot Al_2O_3 \cdot CaCl_2 \cdot 10H_2O$, and it is accepted that this compound forms in concrete exposed to chloride. FS formation provides a sink for chloride and in doing so, may decrease the concentration driving force for the migration of chloride towards embedded steel and also, it has been reported that chloride may bound in calcium silicate hydrate (C-S-H), as a complex oxychloride. Friedel's salt (a chloride-containing AFm phase, $3CaO.Al_2O_3 \cdot CaCl_2 \cdot 10H_2O$), or its high-iron analogue, $C_3F \cdot CaCl_2 \cdot H_{10,}$ form at low temperatures [1–3]. In sulfate-resistant Portland cement, a high amount of alumina is bonded as calcium aluminoferrite, rather than tricalcium aluminate, even at room temperature [4]. It has been reported that the stability of Friedel's salt in chloride contaminated concrete is pH dependant. The solubility of Friedel's salt increases with the degree of atmospheric carbonation of concrete. Ettringite does not exist in severely carbonated concrete as its stability is also pH dependant. Friedel's salt is stable in basic solutions (pH >12), but is destabilized at lower pH values (*e.g.*, by carbonation). Chloride binding of cement is influenced by other factors too; *e.g.*, alkali content appears to have an inhibiting effect on the chloride binding capacity. This fact, however, is overshadowed by a conjoint strong elevation of the OH^- ion concentration in the pore solution, causing a net lowering of the Cl^-/OH^- ratio, which in turn reduces corrosion risk. The threshold chloride content exists for each cement depending on the alkali, C_3A, and aluminoferrite content of the cement [5,6]. Friedel's salt cannot account for all the bound chloride and other products that may bind chloride include calcium silicate hydrate gel (C–S–H) and the ferrite analogue of Friedel's salt [7,8]. However, this latter phase is not considered to be important in a typical Portland cement due to the slow hydration of the ferrite phase [4]. A further mechanism by which chloride can be bound is through the formation of calcium oxychlorides. A number of calcium oxychlorides are known. The existence of $Ca(OH)_2.CaCl_2.H_2O$, the so-called 1:1:1 compound, is well established. Chloride induced corrosion of reinforced concrete is recognized as a primary factor for the deterioration of concrete structures. The threshold value of chloride was estimated as 0.6 to 1.2 kg/m^3 of concrete or 0.15% on the basis of the weight of cement content [9,10]. If the free chloride content is maintained below the threshold value, the rebars will be free from corrosion. In the present investigation, an attempt has been made to explain the relationship between alumina and chloride content on the physical and corrosion resistance properties of concrete.

2. EXPERIMENTAL DETAILS

2.1. Materials

The composition of ordinary Portland cement (OPC) is given in Table 1. Local clean river sand (fineness modulus of medium sand equal to 2.6) conforming to grading zone III of IS:383-1970 was used. Locally available coarse aggregates conforming to graded aggregates of normal size greater than 4.75 mm and less than 16 mm of IS:456-2000 was used. The mix design used was 1:1.8:3.69 with w/c ratio 0.55.

Table 1. Composition of Ordinary Portland Cement (wt%)

Constituents	OPC
SiO_2	24.0 to 25.0
Al_2O_3	1.2 to 1.6
Fe_2O_3	4.4 to 4.8
CaO	62.0 to 63.0
MgO	0.5 to 0.7
SO_3	2.4 to 2.8
LOI	1.5 to 2.0

The grading of fine and coarse aggregates is given in Table 2.

Table 2. Grading of Fine and Coarse Aggregates

Sieve size mm	Coarse aggregate Cumulative weight retained %	Sieve size mm	Fine aggregate Cumulative weight retained %
20.00	0	4.75	0
16.00	25.00	2.26	12.00
12.50	52.00	0.60	49.00
10.00	72.00	0.30	85.00
4.75	100.00	0.15	97.00
---	----	<0.150	100.00

Potable water has been used for making concrete specimens. The admixture used was alumina [Al_2O_3] and calcium chloride [$CaCl_2$]. Thermomechanically (TMT) treated rebar of 12 mm diameter was used as reinforcement.

2.2. Systems Studied

The details of weight of aggregates, cement, water, and admixtures used in each concrete mixture are given in Table 3.

Table 3. Composition of Concrete Mix Design

Cement kg/m^3	Weight of fine aggregate kg/m^3	Weight of coarse aggregate kg/m^3	Water kg/m^3	Alumina kg/m^3	$CaCl_2$ kg/m^3
352	635	1295	194	0	3.52
352	635	1295	194	3.52	3.52
352	635	1295	194	10.56	3.52
352	635	1295	194	17.60	3.52
352	635	1295	194	35.20	3.52
352	635	1295	194	52.80	3.52

2.3. Techniques Studied

2.3.1. Mechanical property of concrete

(i). Compressive strength test

A compressive strength test was carried out as per IS:516-1959 [11] in concrete cubes of size 100 × 100 × 100 mm using 1:1.8:3.69 mix design with W/C ratio of 0.55. Aluminium oxide with varying percentages (1% to 15%) by weight of cement was added during mixing along with 1% $CaCl_2$. During casting, the moulds were mechanically vibrated. After 24 hours, the specimens were removed from the mould and subjected to water curing for 28 days. After curing, the specimens were tested for compressive strength using an AIMIL compression testing machine of 2000 kN capacity at a rate of loading of 140 kN/min. The tests were carried out on triplicate specimens and the average compressive strength values were recorded.

2.3.2. Permeability property of concrete

(i). Rapid chloride permeability test (RCPT)

The resistance to chloride ion penetration in terms of total charge passed in coulombs through concrete specimens after 28 days of water curing was measured as per ASTM C 1202 [12].

(ii). Impressed voltage test

The impressed voltage test has been conducted in the laboratory as an accelerated corrosion testing technique for comparing different characteristics of concrete [13]. Cylindrical concrete specimens of size 50 mm diameter and 100 mm height were cast with 12 mm diameter and 70 mm length rebar embedded in the centre of the concrete specimen. The concrete specimens were cast with and without Al_2O_3 (1% to 15%) along with 1% $CaCl_2$. In this technique, the concrete specimen is immersed in 5% NaCl solution and embedded steel in concrete is made anode with respect to an external stainless steel electrode serving as cathode by applying a constant positive potential of 12 volts to the system from a DC source. The variation of current is recorded with time. A sharp rise in current indicates the onset of corrosion and cracking of the concrete is usually visible thereafter. The time taken for initiation of first crack can be considered as a measure of their relative resistance against chloride permeability and reinforcement corrosion. In the end, concrete specimens were split open and visually examined for rust products. The rebar was cleaned and the weight loss was noted.

2.3.3. Corrosion resistance property

(i). Preparation of rectangular concrete specimens for macrocell corrosion studies

A rectangular concrete specimen of size 279 mm x 152 mm x 114 mm was designed as per ASTM G:109-92 for macrocell corrosion studies. TMT rebar of 12 mm diameter and 300 mm length was used as both anode and cathode in the same concrete. The top mat of rebar acts as anode and the bottom mat of rebar acts as cathode. The anode to cathode area ratio was maintained at 1:2 in order to induce accelerated corrosion. The schematic representation of the macrocell specimen used is given in Figure 1. In both the anode and cathodes, 250 mm length was embedded inside the concrete and the remaining length was used for taking electrical connections with proper insulations. During casting, the concrete specimens were cast with and without Al_2O_3 (1% to 15%) along with 1% $CaCl_2$. The specimens were mechanically vibrated. After 24 hours of setting, the specimens were demoulded and cured in distilled water for 28 days. After curing, the macrocell specimens were subjected to alternate wetting and drying cycles. One cycle consists of 2 weeks of wetting in 3% NaCl solution and 2 weeks of drying. Measurements were carried out during wetting cycles as macrocell current showed maximum magnitude due to the low resistivity of concrete. All the concrete specimens were subjected to 12 complete cycles in the test period.

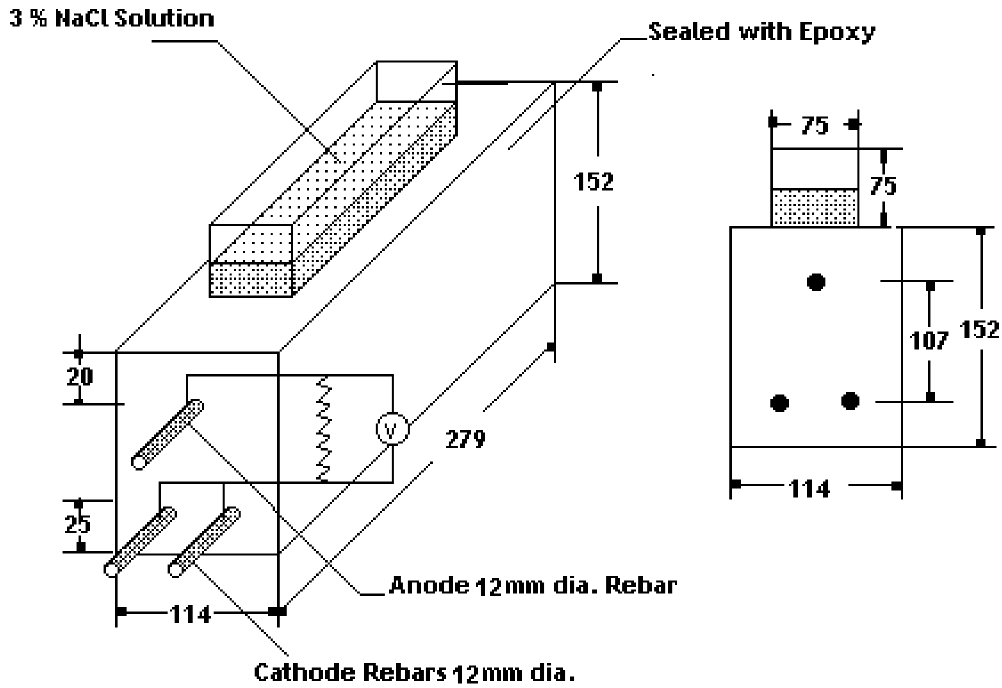

Figure 1: Schematic representation of macrocell corrosion specimen

(ii) Macrocell parameters

Potential vs number of cycles

The open circuit potential of TMT steel anode was monitored for every cycle under alternate wetting and drying conditions using saturated calomel electrode (SCE) as reference electrode.

Macrocell current vs number of cycles

Macrocell current flow between anode and cathode was measured using a high-impedance voltmeter. The top mat and bottom mat rebars were connected by a 100-Ω resistor and macrocell current was obtained from the relation I=V/100. Current was monitored once in every cycle until the average macrocell current measured for the control specimens attained 10 µA or greater. The test was continued up to 12 complete cycles of exposure (12 months) to ensure the presence of sufficient corrosion for visual examination.

Qualitative and quantitative estimation of corrosion

At the end of the exposure period, the concrete specimens were split open and the corrosion rate of TMT steel anodes embedded in concrete specimens was determined by the gravimetric weight loss method. The final weight was measured after cleaning the rebars in inhibited hydrochloric acid as specified in ASTM G1-90. From the initial and final weight, the corrosion rate in mmpy was calculated using the following formula [14]:

$$\text{Corrosion rate} = \frac{87.6 * W}{D * A * T}$$

where W is the metal loss, mg; D the Density of Iron, g/cm^3; A the Area, cm^2; and T is the Time, hours.

Estimation of free chloride contents

The core samples collected near the anode were crushed mechanically and powdered. Then 100 gm of the powdered sample was shaken with 100 ml of double-distilled water in a conical flask using a microid flask shaker for 1 hour. The extract was then filtered through a Whatman filter paper No. 42. The extract prepared from the powdered sample was then analyzed for free chloride contents as per the standard procedures [15,16]. Twenty cc of the filtered solution was taken and the free chloride was estimated by standard silver nitrate using potassium chromate as an indicator. The amount of chloride present was expressed in terms of parts per million (ppm) on the basis of weight of sample taken for analysis.

2.3.4. Surface Examinations

At the end of the exposure period, core samples were cut from the steel-concrete interface and subjected to scanning electron microscopy. A micrograph was recorded using a scanning electron microscope (SEM-HITACHI MODEL, S4800, Japan). Then the samples were crushed mechanically and subjected to x-ray diffraction studies.

3. RESULTS AND DISCUSSION

3.1. Compressive Strength Measurements

Figure 2 shows the compressive strength of OPC concrete with various Al_2O_3 levels at 3, 7, and 28 days of curing. The compressive strength values gradually increased up to 5% Al_2O_3 levels. After that, a slight decrease in compressive strength was observed. The compressive strength data revealed that the addition of Al_2O_3 increased the early strength of concrete. The addition of up to 5% Al_2O_3 showed maximum compressive strength. For example, the compressive strengths at 28 days were 28 MPa, 33 Mpa, and 28 MPa for OPC, OPC+5%Al_2O_3, and OPC+15%Al_2O_3, respectively. These results indicated that added Al_2O_3 interacted with $Ca(OH)_2$ and favored calcium-chloro-aluminate complexes. The formation of such complexes enhanced the compressive strength values up to the 5% Al_2O_3 level. Above 5% Al_2O_3, a decrease in compressive strength values was observed, indicating the optimum level of Al_2O_3 as 5%.

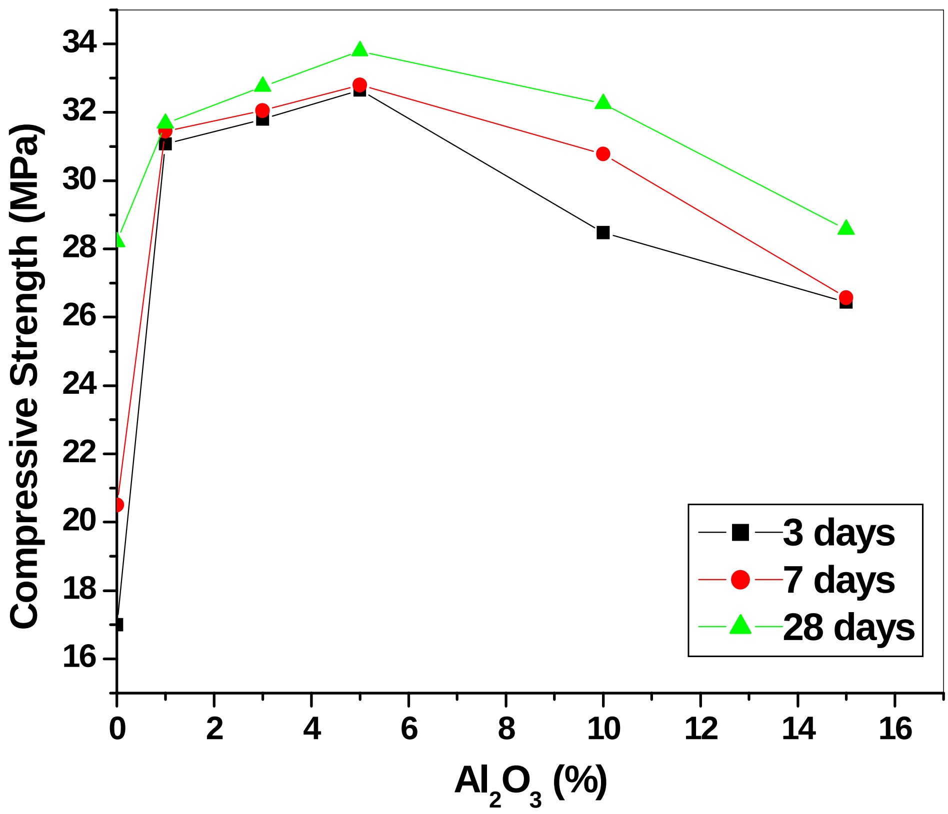

Figure 2: Compressive strength of OPC concrete and various Al_2O_3 additions

3.2. Rapid Chloride Ion Permeability Test (RCPT)

Figure 3 shows the current and coulomb values recorded over 6 hours duration for OPC and OPC concrete with various Al_2O_3 levels. It was observed that at the end of 6 hours, 1083, 1003, 932, 652, 1515, and 3425 coulombs were measured for OPC, 1%, 3%, 5%, 10%, and 15% Al_2O_3 added concrete, respectively. A rapid chloride ion permeability test revealed that the quantity of electrical charge passed for OPC concrete at 5% Al_2O_3 showed a 50% reduction in coulombs. The coulomb value clearly indicated that 5% Al_2O_3 is the critical percentage of addition for fixing of chloride in concrete.

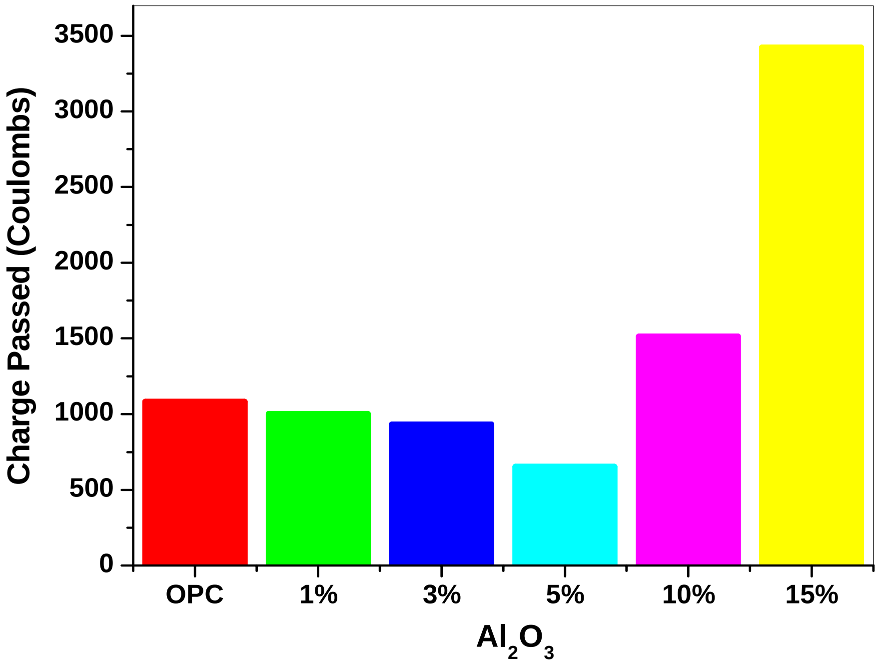

Figure 3: Charge passed in coulombs for OPC concrete and Friedel's salt formation by various Al_2O_3 additions

3.3. Impressed Voltage Test

Table 4 shows the impressed voltage parameters for OPC and OPC with various Al_2O_3 systems. The maximum anodic current and time to first cracking was noted for each system. The average currents recorded were 33 mA, 32 mA, 30 mA, 28 mA, 62 mA, and 75 mA for OPC, 1%, 3%, 5%, 10%, and 15% Al_2O_3 added systems, respectively. From the table, it was observed that beyond the 5% Al_2O_3 addition, there was a sudden shift in current observed and actually doubled for the 10% Al_2O_3 system.

Table 4. Impressed Voltage Parameters for OPC and Friedel's Salt Formation by Various Al_2O_3 Additions

System	Maximum anodic current (mA)	Time to first cracking (days)	Free chloride (ppm)	Corrosion rate (mmpy)
$OPC+1\%CaCl_2+0\%Al_2O_3$	33	7	501	0.0257
$OPC+1\%CaCl_2+1\%Al_2O_3$	32	20	289	0.0129
$OPC+1\%CaCl_2+3\%Al_2O_3$	30	22	209	0.0126
$OPC+1\%CaCl_2+5\%Al_2O_3$	28	24	205	0.0118
$OPC+1\%CaCl_2+10\%Al_2O_3$	62	10	457	0.0266
$OPC+1\%CaCl_2+15\%Al_2O_3$	75	9	633	0.0289

The time taken for initiation of first crack was increased for the 5% Al_2O_3 system. For example, the $OPC+5\%Al_2O_3$ system showed a 3 times increase in the time taken for initiation of first crack when compared to the $OPC+0\%Al_2O_3$ system and a 2 times increase when compared to the $OPC+10\%Al_2O_3$ system. The average corrosion rate for steel embedded in OPC concrete was found to be 0.0257 mmpy. The lowest corrosion rate was observed for steel embedded in the $OPC+5\%Al_2O_3$ system. The 12V impressed voltage test indicated a gradual increase in anodic current flow and delayed time taken for initial crack up to 5% Al_2O_3 addition, indicating the critical percentage with improved corrosion resistance properties of concrete.

3.4. Macrocell Corrosion Studies

The electrochemical characteristics of the half-cell potential of steel measured periodically against a SCE with time for various systems are shown in Figure 4. It was observed from Figure 4 that steel embedded in OPC control concrete showed active condition within 6 cycles of exposure. On the other hand, OPC with various Al_2O_3 levels up to 5% maintained its passive condition of embedded steel throughout the exposure period of 12 months. However, OPC with 10% and 15% Al_2O_3 levels showed active condition within 4 cycles of exposure. These results indicated that steel embedded in OPC concrete up to 5% Al_2O_3 performed better under macrocell conditions. The better corrosion resistance performance of steel embedded in 5% Al_2O_3 added concrete is due to the fact that the added Al_2O_3 phases reacted with free lime in concrete and formed calcium chloroaluminate complexes, which in turn considerably reduced the permeability of chloride and improved the corrosion resistance property of embedded steel in concrete.

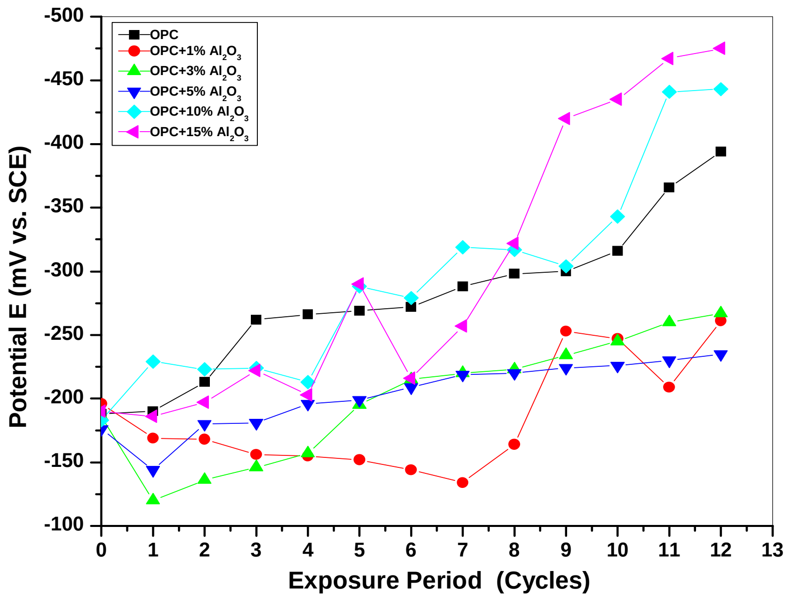

Figure 4: Potential – time behavior of steel embedded in OPC and Friedel's salt formation by various Al_2O_3 additions

The macro Sami A. Al-Marshoud <SAMARSHOUD@se.com.sa>cell currents or galvanic currents measured periodically with time for steel in OPC and with various Al_2O_3 levels are shown in Figure 5.

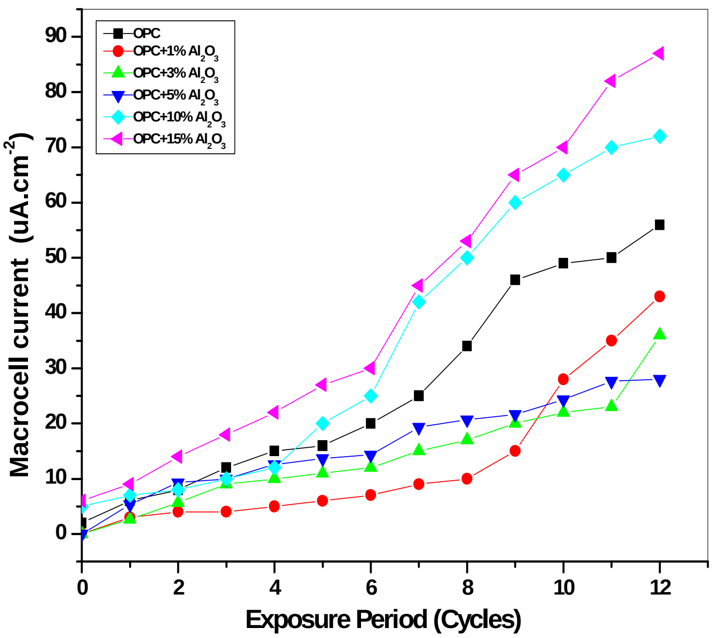

Figure 5: Macrocell current vs exposure period for OPC and Friedel's salt formation by various Al_2O_3 additions

Here again, it was proved that OPC concrete containing 5% Al_2O_3 level showed the minimum current flow of 28 μA even after 12 cycles of exposure. On the other hand, the macrocell current is tremendously increased by 2.5 times and 3 times for the 10% Al_2O_3 level and the 15% Al_2O_3 level, respectively. At higher percentages of Al_2O_3 (10% and 15%) the unreacted Al_2O_3 phases were leached out and increased the permeability of chloride. With this result, a considerable increase in the magnitude of macrocell current was measured.

The estimated free chloride contents and the corrosion rate of embedded steel for various systems is given in Table 5. The free chloride contents estimated for OPC concrete was found to be 1667 ppm. The addition of Al_2O_3 considerably reduced the free chloride contents. For example, at 5% Al_2O_3, a nearly 3 times decrease in free chloride contents was observed. The corrosion rate for the OPC system was found to be 0.2366 mmpy. The addition of Al_2O_3 considerably reduced the corrosion rate. For example, at 5% Al_2O_3 level, a 2 times decrease in corrosion rate was observed. These results clearly proved that 5% Al_2O_3 addition effectively enhanced the corrosion resistance properties of embedded steel in concrete.

Table 5. Free Chloride Contents and Corrosion Rate of Steel Under Macrocell Conditions for OPC and Friedel's Salt Formation by Various Al_2O_3 Additions

Systems	Free chloride contents (ppm)	Corrosion rate (mmpy)
OPC+1%$CaCl_2$+ 0%Al_2O_3	1667	0.2366
OPC+1%$CaCl_2$+1%Al_2O_3	813	0.1189
OPC+1%$CaCl_2$+3%Al_2O_3	750	0.1187
OPC+1%$CaCl_2$+5%Al_2O_3	557	0.1181
OPC+1%$CaCl_2$+10%Al_2O_3	929	0.1611
OPC+1%$CaCl_2$+15%Al_2O_3	962	0.1621

3.5. Scanning Electron Microscopy

Figures 6(a to d) show the micrographs for Friedel's salt formation at 1%, 3%, 5%, and 10% Al_2O_3 levels, respectively. Micrographs showed a gradual formation of Friedel's salt at all the Al_2O_3 levels. However, a denser formation of Friedel's salt complexes was noticed at the 5% Al_2O_3 level. The appearance of the Friedel's salt formation is white solid and is marked in the micrograph.

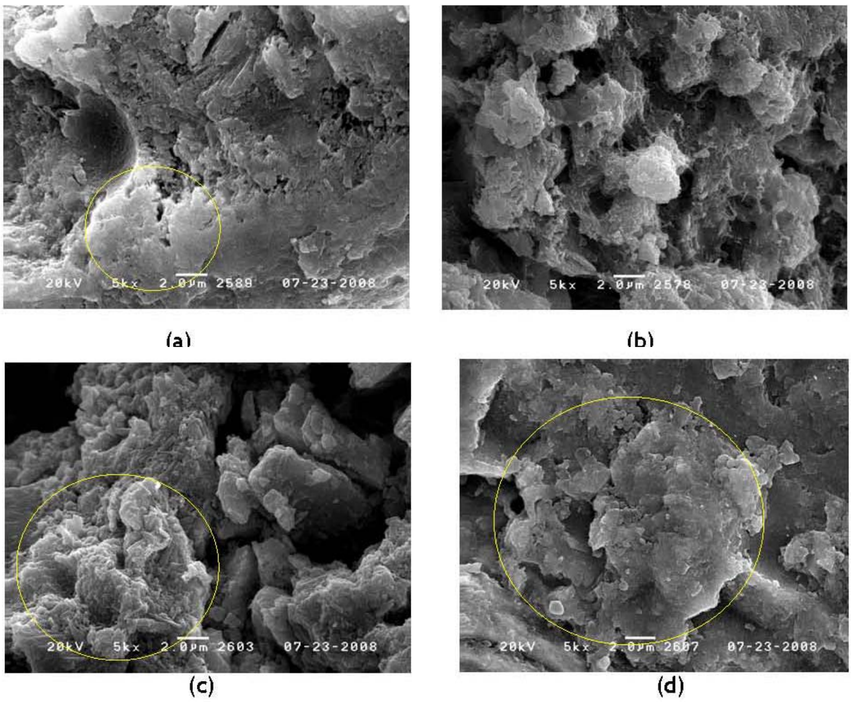

Figure 6: Scanning electron micrograph for core concrete specimen at various Al_2O_3 levels
(a).OPC+1% $CaCl_2$+ 1% Al_2O_3 ; (b).OPC +1% $CaCl_2$ +3% Al_2O_3
(c).OPC+1% $CaCl_2$+ 5% Al_2O_3 ; (d).OPC +1% $CaCl_2$ +10% Al_2O_3

3.6. X-Ray Diffraction

Figure 7 shows the XRD pattern for Friedel's salt formation at 5% Al_2O_3 level. The XRD pattern at 5% Al_2O_3 level confirmed the existence of a greater amount of Friedel's salt [17,18]. Above all, the optimum percentage of alumina for the formation of Friedel's salt in OPC concrete with improved properties was found to be 5%.

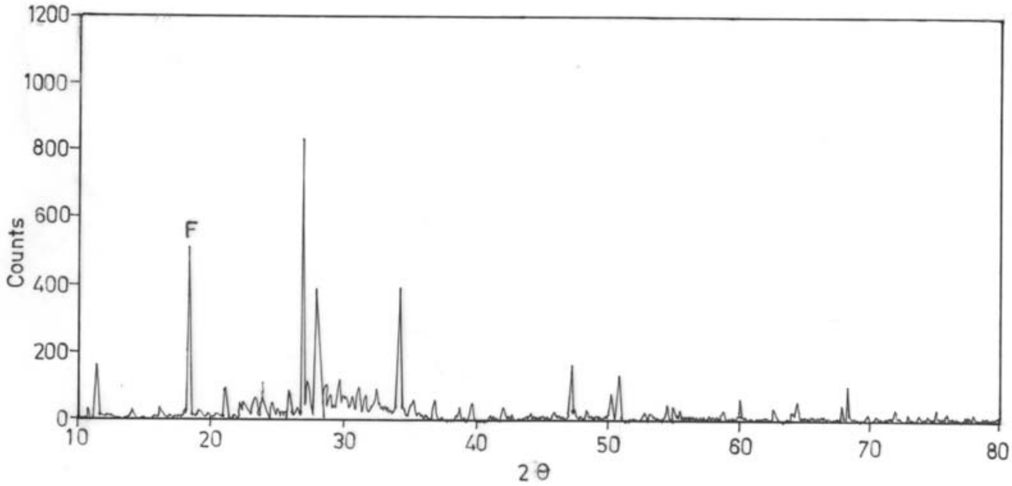

Figure 7: XRD pattern of Friedel's salt (OPC+1% $CaCl_2$+ 5% Al_2O_3)
F: formation of Friedel's salt

4. CONCLUSIONS

The addition of up to 5% Al_2O_3 showed maximum compressive strength. A Rapid Chloride Ion Permeability Test (RCPT) revealed that the quantity of electrical charge passed for OPC concrete at 5% Al_2O_3 showed a 50% reduction in coulombs. The 12V impressed voltage test indicated a gradual increase in anodic current flow and delayed time taken for initial crack up to 5% Al_2O_3 addition. Potential *vs* time data in macrocell corrosion studies maintained the passivity of steel embedded in OPC concrete up to 5% Al_2O_3 throughout the exposure period of 12 months. Macrocell current is tremendously increased by 2.5 times and 3 times for 10% Al_2O_3 level and 15% Al_2O_3 level, respectively. The addition of higher percentages of Al_2O_3 (10% and 15%) leads to the formation of a coarser pore structure, thereby leading to an increase in the porosity of concrete resulting in increased permeability and decreased corrosion resistance. Scanning electron micrographs revealed a denser formation of Friedel's salt at the 5% Al_2O_3 level. The XRD pattern at the 5% Al_2O_3 level also confirmed the existence of a greater amount of Friedel's salt.

ACKNOWLEDGMENTS

The authors thank the Director, CECRI, Karaikudi and Council of Scientific and Industrial Research (CSIR), New Delhi for kind permission to publish this article. The authors also gratefully acknowledge the support of the Center for Concrete Corea, South Korea, for financial assistance.

REFERENCES

[1] V. S. Batra, "A Boon to Concrete Construction", *Indian Concrete Journal*, **65**(1991), p. 247.

[2] V. S. Bharadhwaj, V. S. Batra, and V. V. Sastry, "Effects of Admixtures on Pozzolona Concrete", *Indian Concrete Journal*, **55**(1981), p. 193.

[3] R. G. Limaye, "Admixtures for High Strength Concrete", *Indian Concrete Journal*, **50**(1996), p. 1.

[4] N. P. Mailvaganam, "Admixtures in Concrete- An Overview", *Indian Concrete Journal*, **36**(1991), p. 1.

[5] Ha-Won Song, V. Saraswathy, S. Muralidharan, and K. Thangavel, "Tolerance Limit of Chloride for Steel in Blended Cement Mortar Using the Cyclic Polarisation Technique", *J. Appl. Electrochem*., **38**(2008), p. 445.

[6] Ha-Won Song, V. Saraswathy, S. Muralidharan, Chang-Hong Lee, and K. Thangavel, "Role of Alkaline Nitrites in the Corrosion Performance of Steel in Composite Cements", *J. Appl. Electrochem*., **39**(2009), p. 15.

[7] Marc Jolin, Denis Beaupre, Michel Pigeon, and Ann Lamontagne, "Use of Set Accelerating Admixtures in Dry Mix Shortcrete", *Journal of Material in Civil Engineering*, **40**(1997), p. 1.

[8] G. Morconi, F. Titarelli, and V. Corinaldesi, "Review of Silicone Based Hydrophobic Treatment and Admixtures for Concrete", *Indian Concrete Journal*, **78**(2002), p. 25.

[9] S. E. Hussain, Rasheeduzzafar, A. Al-Musallam, and A. S. Al-Gahtani, "Factors Affecting Threshold Chloride for Reinforcement Corrosion in Concrete", *Cement and Concrete Research*, **25**(1995), pp. 1543–1555.

[10] Marco Manera, Øystein Vennesland, and Luca Bertolini, "Chloride Threshold for Rebar Corrosion in Concrete With Addition of Silica Fume", *Corrosion Science*, **50**(2008), pp. 554–560.

[11] "Determination of Compressive Strength of Concrete", IS:516–1959.

[12] ASTM C1202 – 09; "Standard Test Method for Electrical Indication of Concrete's Ability to Resist Chloride Ion Penetration".

[13] "Florida Method of Test for an Accelerated Laboratory Method for Corrosion Testing of Reinforced Concrete Using Impressed Current", FM 5-522, September 2000.

[14] M. G. Fontana, *Corrosion Engineering, 3rd Edition*. New York: McGraw Hill, 1986, p. 173.

[15] M. N. Haque and O. A. Kayyali, *ACI Materials J.*, **92**(1995), p. 532.

[16] K. Thangavel, T. M. Balasubramanian, and N. S. Rengaswamy, *Indian Concrete Journal*, April (2000), p. 203.

[17] James V. Bothe Jr. and Paul W. Brown, "PhreeqC Modeling of Friedel's Salt Equilibria at $23\pm1^{o}C$", *Cement and Concrete Research*, **34**(2004), p. 1057.

[18] G. Renaudin, J. P. Rapin, E. Elkaim, and M. Francois, "Polytypes and Polymorphs in the Related Friedel's Salt $[Ca_2Al(OH)6]^{\pm}[X.2H_2O]$ Halide Series", *Cement and Concrete Research*, **34**(2004), pp. 1845–1852.